Osmotic self-propulsion of slender particles

Ory Schnitzer[1] and Ehud Yariv[2]

[1)] *Department of Mathematics, Imperial College London, South Kensington Campus, SW7 2AZ, London, United Kingdom*

[2)] *Department of Mathematics, Technion — Israel Institute of Technology, Haifa 32000, Israel*

(Dated: 9 February 2015)

We consider self-diffusiophoresis of axisymmetric particles using the continuum description of Golestanian *et al.* [New J. Phys. **9**, 126 (2007)] where the chemical reaction at the particle boundary is modelled by a prescribed distribution of solute absorption and the interaction of solute molecules with that boundary is represented by diffusio-osmotic slip. With a view towards modelling of needle-like particle shapes, commonly employed in experiments, the self-propulsion problem is analyzed using slender-body theory. For a particle of length $2L$ whose boundary is specified by the axial distribution $\kappa(z)$ of cross-sectional radius, we obtain the following approximation for the particle velocity,

$$-\frac{\mu}{2DL}\int_{-L}^{L} j(z)\frac{d\kappa(z)}{dz}\,dz,$$

wherein $j(z)$ is the solute-flux distribution, μ the diffusio-osmotic slip coefficient, and D the solute diffusivity. This approximation can accommodate discontinuous flux distributions, which are commonly used for describing bimetallic particles; it agrees strikingly well with the numerical calculations of Popescu *et al.* [Eur. Phys. J. E Soft Matter **31**, 351–367 (2010)], performed for spheroidal particles.

Chemical self-propulsion of a micron-size particle results from a solute-consuming catalysis or solute-producing polymerization at the particle boundary through the interaction of the solute molecules with that boundary. This self-propulsion mechanism, originally demonstrated in the experiments of Paxton *et al.*,[1] has attracted significant attention in the physics, chemistry, and engineering communities, resulting in extensive modelling[2,3] and experimental[4,5] efforts. When the solute is electrically neutral and sufficiently dilute, its short-range interaction with the particle boundary may be represented by a simple diffusio-osmotic slip condition,[6] relating the velocity jump across the interaction layer to the tangential gradient of solute concentration. A simple model of such a slip-based self-diffusiophoresis was provided by Golestanian *et al.*,[3] who for simplicity described the chemical reaction by a prescribed distribution of solute flux. A different "colloidal" description, using the osmotic-pressure concept, was provided by Córdova-Figueroa *et al.*;[7] the linkage between the colloidal and continuum approaches was discussed by Brady[8] and Córdova-Figueroa *et al.*[9]

In experimental demonstrations of chemical self-propulsion it is common to employ rod-like particles.[1,10–12] It is therefore desirable to derive approximations for the speed acquired by elongated shapes.[1,3,10,13] In this letter we accomplish this by applying slender-body techniques within the slip-based continuum framework of Golestanian *et al.*[3] The methodology used herein resembles that employed in the slender-body analysis of an electrokinetic model of self-propulsion.[14]

We consider an axisymmetric particle of length $2L$ and characteristic width a which is suspended in a viscous liquid. In the continuum description of Golestanian *et al.*[3] the catalytic reaction on the particle boundary is represented by a prescribed flux of solute into the boundary, say of typical magnitude α. In that description solute transport is purely diffusive,[15] governed by the solute diffusivity D. We use a dimensionless notation where length variables are normalized by L; the excess-solute concentration c, relative to the ambient concentration, by $\mathcal{C} = \alpha a/D$; and velocities by $\mu\mathcal{C}/L$, μ being the (uniform) diffusio-osmotic slip coefficient. Our goal is the calculation of the particle velocity $\mathcal{U}$ relative to the otherwise quiescent liquid.

The governing equations are written using a particle-fixed cylindrical coordinate system, with the z-axis lying along the particle symmetry axis: see Fig. 1. The particle boundary is given by

$$r = \epsilon\kappa(z) \quad \text{for} \quad -1 < z < 1, \tag{1}$$

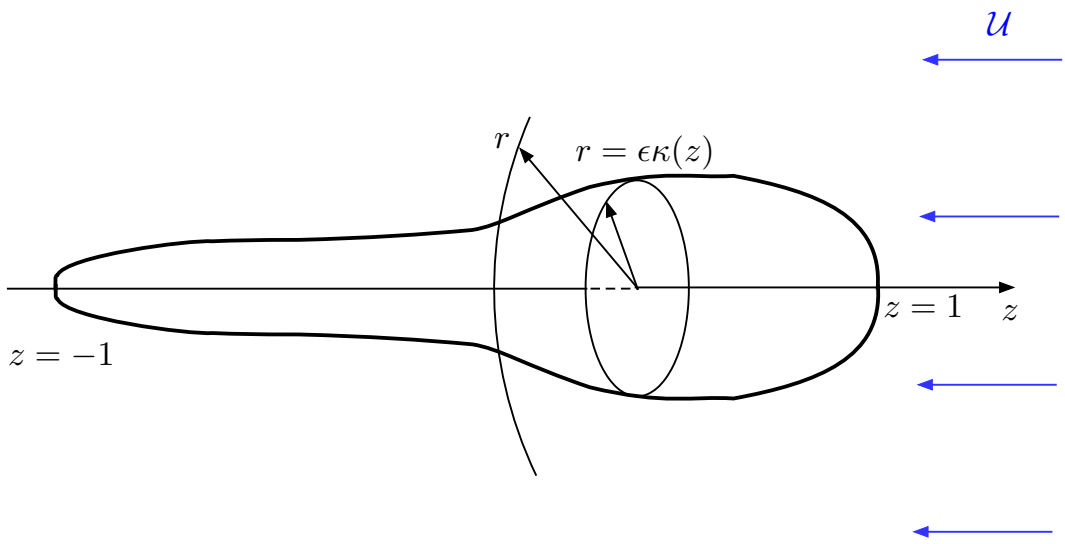

FIG. 1. Schematic of the particle geometry and cylindrical coordinates.

where r is the radial coordinate, and $\epsilon = a/L$ is the particle slenderness. With these definitions, the shape function $\kappa(z)$ is $O(1)$; we impose, with no loss of generality,

$$\kappa(0) = 1. \tag{2}$$

In addition, $\kappa(z)$ satisfies the end conditions

$$\kappa(\pm 1) = 0. \tag{3}$$

The excess-solute concentration is governed by Laplace's equation

$$\nabla^2 c = 0 \quad \text{for} \quad r > \epsilon\kappa(z), \tag{4}$$

the imposed-flux condition

$$\frac{\partial c}{\partial n} = \epsilon^{-1} j(z) \quad \text{at} \quad r = \epsilon\kappa(z), \tag{5}$$

where $j(x)$ is the inward solute flux, normalized by α, and the decay requirement,

$$c \to 0 \quad \text{as} \quad r^2 + z^2 \to \infty. \tag{6}$$

The flow field is governed by the continuity and Stokes equations. It is engendered by the diffusio-osmotic slip condition

$$\mathbf{u} = \boldsymbol{\nabla}_s c \quad \text{at} \quad r = \epsilon\kappa(z), \tag{7}$$

in which $\boldsymbol{\nabla}_s$ is the surface-gradient operator, and the far-field approach to a uniform stream,

$$\mathbf{u} \to -\mathcal{U}\hat{\mathbf{k}} \quad \text{as} \quad r^2 + z^2 \to \infty, \tag{8}$$

$\hat{\mathbf{k}}$ being a unit vector in the z-direction. The self-propulsion speed $\mathcal{U}$ is set by requiring the particle to be force free.

We now consider the slender limit $\epsilon \ll 1$ using inner–outer asymptotic expansions.[16] The "outer" region, with r fixed as $\epsilon \to 0$, describes transport on the longitudinal scale, where the particle appears as a zero-thickness line segment of length 2. The "inner" region, where $r = O(\epsilon)$ as $\epsilon \to 0$, describes transport on the cross-sectional scale, where the particle appears as an infinite cylinder of a quasi-uniform radius. The latter limit is facilitated by the introduction of the stretched radial coordinate $\rho = r/\epsilon$. In terms of this inner coordinate the particle boundary is $\rho = \kappa(z)$, while the normal-derivative and surface-gradient operators adopt the respective forms

$$\frac{\partial}{\partial n} \approx \frac{1}{\epsilon}\frac{\partial}{\partial \rho}, \quad \boldsymbol{\nabla}_s \approx \hat{\mathbf{k}}\left(\frac{\partial}{\partial z} + \frac{d\kappa}{dz}\frac{\partial}{\partial \rho}\right). \tag{9}$$

Hereafter, the approximation symbol '$\approx$' implies a relative error which is at least as small as some positive power of ϵ, and is accordingly smaller than any power of $1/\ln\epsilon$.

We begin with the calculation of c. In the inner region, condition (5) in conjunction with (9) suggests the expansion $c \approx \bar{c}(\rho, z; \epsilon) + \cdots$, wherein $\bar{c}$ is allowed to depend logarithmically upon ϵ. This variable is governed by the leading-order balance of Laplace's equation,

$$\frac{\partial}{\partial \rho}\left(\rho\frac{\partial \bar{c}}{\partial \rho}\right) = 0 \quad \text{for} \quad \rho > \kappa(z), \tag{10}$$

and the imposed-flux condition (5), namely

$$\frac{\partial \bar{c}}{\partial \rho} = j(z) \quad \text{at} \quad \rho = \kappa(z). \tag{11}$$

The solution of (10)–(11) is

$$\bar{c} = C(z; \epsilon) + j(z)\kappa(z)\ln\rho, \tag{12}$$

where the integration "constant" C is determined by matching with the outer solution.

In the outer region we write $c \approx \tilde{c}(r, z) + \cdots$, where $\tilde{c}$ is represented as a line distribution of sources

$$\tilde{c} = \int_{-1}^{1} \frac{s(\zeta)\, d\zeta}{\sqrt{r^2 + (z-\zeta)^2}}, \tag{13}$$

which automatically satisfies Laplace's equations (4) and the attenuation condition (6). The source intensity $s(z)$ is determined by asymptotic matching with the inner solution. To this end we employ the small-r approximation of (13),[17]

$$\tilde{c} = 2s(z) \ln \frac{2\sqrt{1-z^2}}{r} + \int_{-1}^{1} \frac{s(\zeta) - s(z)}{|\zeta - z|} \, d\zeta + O(r^2). \tag{14}$$

Performing the matching we readily find that $s(z) = -j(z)\kappa(z)/2$, and hence

$$C(z;\epsilon) = C_{-1}(z) \ln \frac{1}{\epsilon} + C_0(z), \tag{15}$$

wherein $C_{-1}(z) = -j(z)\kappa(z)$ and

$$C_0(z) = -j(z)\kappa(z) \ln(2\sqrt{1-z^2}) - \frac{1}{2} \int_{-1}^{1} \frac{j(\zeta)\kappa(\zeta) - j(z)\kappa(z)}{|\zeta - z|} \, d\zeta. \tag{16}$$

Using (12) and (15) we obtain

$$\left(\frac{\partial c}{\partial z} + \frac{d\kappa}{dz} \frac{\partial c}{\partial \rho} \right)_{\rho = \kappa(z)} \approx \ln(1/\epsilon) W_{-1}(r,z) + W_0(r,z) \stackrel{\text{def}}{=} W(z;\epsilon), \tag{17}$$

wherein

$$W_{-1} = \frac{dC_{-1}}{dz}, \quad W_0 = \frac{dC_0}{dz} + \ln \kappa(z) \frac{d}{dz} \left[j(z)\kappa(z) \right] + j(z) \frac{d\kappa}{dz}. \tag{18}$$

In particular, use of (3) implies that

$$\int_{-1}^{1} W_{-1}(z) \, dz = 0. \tag{19}$$

We now proceed to the calculation of the velocity field. In particular, we consider the axial velocity component w. Its inner and outer expansions are $w \approx \bar{w}(\rho, z; \epsilon) + \cdots$ and $w \approx \tilde{w}(r, z; \epsilon) + \cdots$, respectively, in which $\bar{w}$ and $\tilde{w}$ are allowed to depend weakly on ϵ. In the inner region, the general axisymmetric solution of the degenerated Stokes equations is well known.[16] Imposing the slip condition $\bar{w} = W$ at $\rho = \kappa(z)$ [see (17)], the axial velocity component reads

$$\bar{w} = W(z;\epsilon) + A(z;\epsilon) \ln \frac{\rho}{\kappa(z)}, \tag{20}$$

where we allow A to depend weakly on ϵ through an expansion in inverse powers of $\ln(1/\epsilon)$,

$$A(z;\epsilon) = A_0(z) + \frac{1}{\ln(1/\epsilon)} A_1(z) + \cdots. \tag{21}$$

In the outer region, the disturbance relative to the uniform stream is represented by a line-singularity distribution of Stokeslets,

$$\tilde{w} + \mathcal{U} = \int_{-1}^{1} \mathcal{F}(\zeta;\epsilon) \left\{ \frac{1}{[r^2 + (z-\zeta)^2]^{1/2}} + \frac{(z-\zeta)^2}{[r^2 + (z-\zeta)^2]^{3/2}} \right\} d\zeta, \tag{22}$$

wherein the force density $\mathcal{F}(z;\epsilon)$ possesses an expansion in inverse powers of $\ln(1/\epsilon)$,

$$\mathcal{F}(z;\epsilon) = \mathcal{F}_0(z) + \frac{1}{\ln(1/\epsilon)}\mathcal{F}_1(z) + \cdots ; \tag{23}$$

we note that at small r the right-hand side of (22) is

$$4\mathcal{F}(z;\epsilon)\ln\frac{2\sqrt{1-z^2}}{r} - 2\mathcal{F}(z;\epsilon) + 2\int_{-1}^{1}\frac{\mathcal{F}(\zeta;\epsilon)-\mathcal{F}(z;\epsilon)}{|\zeta - z|}\,d\zeta + O(r^2). \tag{24}$$

The particle speed $\mathcal{U}$ is set by the force-free condition

$$\int_{-1}^{1}\mathcal{F}(z;\epsilon)\,dz = 0. \tag{25}$$

In view of expansion (23), this is tantamount to an infinite sequence of conditions governing $\{\mathcal{F}_n\}_{n=0}^{\infty}$. Since the slip expression (17) begins at $O(\ln\epsilon)$, it is plausible to postulate an expansion for the particle speed that begins at this asymptotic order:

$$\mathcal{U} = \ln(1/\epsilon)\,\mathcal{U}_{-1} + \mathcal{U}_0 + \frac{1}{\ln(1/\epsilon)}\mathcal{U}_1 + \cdots . \tag{26}$$

Performing the asymptotic matching using an intermediate variable[18] we readily obtain $A_n(z) = -4\mathcal{F}_n(z)$ for all n. Leading-order matching at $O(\ln\epsilon)$ yields $\mathcal{F}_0(z) = [\mathcal{U}_{-1} + W_{-1}(z)]/4$. Application of (25) and use of (19) thus yields $\mathcal{U}_{-1} = 0$. The large leading-order slip does not result in a comparable self-propulsion speed.

We therefore need to go to $O(1)$ at the matching process, where we obtain

$$\mathcal{U}_0 + W_0(z) - 4\mathcal{F}_1(z) = W_{-1}(z)\ln\frac{2\sqrt{1-z^2}}{\kappa(z)} - \frac{1}{2}W_{-1}(z) + \frac{1}{2}\int_{-1}^{1}\frac{W_{-1}(\zeta)-W_{-1}(z)}{|\zeta - z|}\,d\zeta, \tag{27}$$

which serves as an equation governing $\mathcal{F}_1$. Application of (19) and (25) yields here

$$\mathcal{U}_0 = \frac{1}{2}\int_{-1}^{1}W_{-1}(z)\ln\frac{2\sqrt{1-z^2}}{\kappa(z)}\,dz - \frac{1}{2}\int_{-1}^{1}W_0(z)\,dz. \tag{28}$$

Substitution of (18) followed by integration by parts in conjunction with (3) and (16) yields the remarkably simple approximation

$$\mathcal{U}_0 = -\frac{1}{2}\int_{-1}^{1}j(z)\frac{d\kappa}{dz}\,dz, \tag{29}$$

whose dimensional version is provided in the abstract.

In modelling realistic inhomogeneous swimmers, which are typically composed of two different metallic segments (e.g. gold and platinum), it is common[19] to employ a discontinuous

distribution of chemical activity, say $j(z) = 1$ for $z > 0$ and 0 for $z < 0$. Making use of (2)–(3) then yields the result

$$\mathcal{U}_0 = \frac{1}{2}, \tag{30}$$

which is independent of the particle shape. Expression (30) can be compared with the numerical calculations of Popescu *et al.*[13] for spheroidal particles with the same janus-type flux distribution. The smallest value of ϵ for which results are provided in Fig. 4(a) of Ref. 13 is about 0.1; in the present notation, the corresponding value of $\mathcal{U}$ is visually interpreted as about 0.48 — a remarkable agreement with (30). Given the $O(1/\ln\epsilon)$ relative error in (30) and the moderate slenderness value used in the above comparison, this agreement may actually appear too good to be true. To understand it, we perform asymptotic matching at the next order, $O(1/\ln\epsilon)$, obtaining the velocity correction

$$\mathcal{U}_1 = 2\int_{-1}^{1} \mathcal{F}_1(z) \ln\frac{2\sqrt{1-z^2}}{\kappa(z)}\, dz. \tag{31}$$

In principle, substitution of $\mathcal{F}_1(z)$ as provided by (27) would result in (a rather complicated) expression for the velocity correction. In the particular case of spheroids, however, the integral appearing in (31) vanishes due to (25), whereby $\mathcal{U}_1 = 0$. In fact, it is readily verified that this is the case at all subsequent asymptotic orders. We conclude that in the particular case of a spheroid $\mathcal{U} = \mathcal{U}_0$ with an algebraic error, thus explaining the agreement with Popescu *et al.*[13]

Our derivation of (30), which is independent of particle shape, hinges upon condition (3). This constraint does not preclude straight rods which can be represented by shape functions dropping to 0 at $z = \pm 1$ rapidly but smoothly. If that is not the case, a systematic scheme requires accounting for end effects. In this context, we note that our approximation fundamentally differs from the formula obtained by Golestanian *et al.*[3] in the case of a cylindrical rod: see Eq. (16) in that paper. In fact, that formula does not resemble at all the more primitive expression (29) obtained herein. We could not understand the manner by which Golestanian *et al.*[3] have obtained their formula. Equation (14) in Ref. 3, which underlies it, appears to be a meaningless interpretation of a line-singularity representation, as it involves an integral that does not exist.

We suspect that the erroneous formula in Golestanian *et al.*[3] is a consequence of an attempt to apply an intuitive approach in a delicate situation where the diffuso-osmotic slip and self-propulsion speed are not of the same asymptotic order. In that sense, this is quite an

exceptional slender-body problem. An important consequence of the logarithmically large slip is that the leading-order outer velocity induced by the particle,

$$\frac{1}{4}\hat{\mathbf{k}}\cdot\int_{-1}^{1} W_{-1}(\zeta)\left(\frac{\mathsf{I}}{|\mathbf{x}'|}+\frac{\mathbf{x}'\mathbf{x}'}{|\mathbf{x}'|^3}\right)d\zeta \tag{32}$$

(I being the idemfactor, $\mathbf{x}'=\mathbf{x}-\zeta\hat{\mathbf{k}}$), is of the same order as the particle velocity. This implies unusually strong $O(1)$ hydrodynamic interactions. Considering large $|\mathbf{x}|$, (32) degenerates to the stresslet[20] flow $\mathsf{S}:\mathbf{xxx}/|\mathbf{x}|^5$, wherein

$$\mathsf{S}=\frac{1}{4}(3\hat{\mathbf{k}}\hat{\mathbf{k}}-\mathsf{I})\int_{-1}^{1} j(\zeta)\kappa(\zeta)\,d\zeta. \tag{33}$$

Last, the standard modelling in the literature of auto-diffusiophoresis involves a fore–aft symmetric particle shape (e.g. spheres[19] and spheroids[13]) where the preferred direction for motion is set by an asymmetric distribution of chemical reaction. It was noted however by Shklyaev *et al.*[21] that homogeneous particles can also undergo chemical locomotion, provided that their shape is fore–aft asymmetric.[22] Shklyaev *et al.*[21] demonstrated this concept for such axisymmetric particles, using a combination of approximation methods for small deviation from sphericity and numerical methods for finite non-sphericity.

Unsurprisingly, the swimming speed found by Shklyaev *et al.*[21] for nearly-spherical particles turned out to be small, proportional to the square of the distortion from sphericity. Practical interest thus lies in finite non-sphericity. The present scheme may be readily applied to study such homogeneous asymmetric particles. Setting $j\equiv 1$ in (29) in conjunction with (3) results in a trivial approximation. The particle velocity in this case is therefore $O(1/\ln\epsilon)$; it may be obtained by substituting $\mathcal{F}_1$, as provided by (27), into (31).

REFERENCES

[1]W. F. Paxton, K. C. Kistler, C. C. Olmeda, A. Sen, S. K. S. Angelo, Y. Cao, T. E. Mallouk, P. E. Lammert, and V. H. Crespi, "Catalytic nanomotors: autonomous movement of striped nanorods," J. Am. Chem. Soc **126**, 13424–13431 (2004).

[2]R. Golestanian, T. B. Liverpool, and A. Ajdari, "Propulsion of a molecular machine by asymmetric distribution of reaction products," Phys. Rev. Lett. **94**, 220801 (2005).

[3]R. Golestanian, T. B. Liverpool, and A. Ajdari, "Designing phoretic micro-and nano-swimmers," New J. Phys. **9**, 126 (2007).

[4]S. J. Ebbens and J. R. Howse, "Direct observation of the direction of motion for spherical catalytic swimmers," Langmuir **27**, 12293–12296 (2011).

[5]S. Ebbens, M.-H. Tu, J. R. Howse, and R. Golestanian, "Size dependence of the propulsion velocity for catalytic janus-sphere swimmers," Phys. Rev. E **85**, 020401 (2012).

[6]J. L. Anderson, M. E. Lowell, and D. C. Prieve, "Motion of a particle generated by chemical gradients. Part 1. Non-electrolytes," J. Fluid Mech. **117**, 107–121 (1982).

[7]U. M. Córdova-Figueroa and J. F. Brady, "Osmotic propulsion: The osmotic motor," Phys. Rev. Lett. **100**, 158303 (2008).

[8]J. F. Brady, "Particle motion driven by solute gradients with application to autonomous motion: continuum and colloidal perspectives," J. Fluid Mech. **667**, 216–259 (2011).

[9]U. M. Córdova-Figueroa, J. F. Brady, and S. Shklyaev, "Osmotic propulsion of colloidal particles via constant surface flux," Soft Matter **9**, 6382–6390 (2013).

[10]W. F. Paxton, A. Sen, and T. E. Mallouk, "Motility of catalytic nanoparticles through self-generated forces," Chem. — Eur. J. **11**, 6462 (2005).

[11]G. A. Ozin, I. Manners, S. Fournier-Bidoz, and A. Arsenault, "Dream nanomachines," Adv. Mater. **17**, 3011–3018 (2005).

[12]S. Fournier-Bidoz, A. C. Arsenault, I. Manners, and G. A. Ozin, "Synthetic self-propelled nanorotors," Chemical Communications **2005**, 441–443 (2005).

[13]M. N. Popescu, S. Dietrich, M. Tasinkevych, and J. Ralston, "Phoretic motion of spheroidal particles due to self-generated solute gradients," Eur. Phys. J. E Soft Matter **31**, 351–367 (2010).

[14]E. Yariv, "Electrokinetic self-propulsion by inhomogeneous surface kinetics," Proc. Roy. Soc. London A **467**, 1645 (2011).

[15]The role of solute advection was discussed by Michelin & Lauga[19] and Yariv & Michelin[23].

[16]R. G. Cox, "The motion of long slender bodies in a viscous fluid. Part 1. General theory," J. Fluid Mech. **44**, 791–810 (1970).

[17]G. K. Batchelor, "Slender-body theory for particles of arbitrary cross-section in Stokes flow," J. Fluid Mech. **44**, 419–441 (1970).

[18]E. J. Hinch, *Perturbation Methods* (Cambridge University Press, Cambridge, 1991).

[19]S. Michelin and E. Lauga, "Phoretic self-propulsion at finite Péclet numbers," J. Fluid Mech. **747**, 572–604 (2014).

[20]G. K. Batchelor, "The stress system in a suspension of force-free particles," J. Fluid Mech.

41, 545–570 (1970).

[21]S. Shklyaev, J. F. Brady, and U. M. Córdova-Figueroa, "Non-spherical osmotic motor: chemical sailing," J. Fluid Mech. **748**, 488–520 (2014).

[22]Michelin *et al.*[24] showed a different mechanism of self-propulsion of homogeneous spheres, driven by an instability associated with nonlinear solute advection.

[23]E. Yariv and S. Michelin, "Phoretic self-propulsion at large Péclet numbers," J. Fluid Mech.(Submitted).

[24]S. Michelin, E. Lauga, and D. Bartolo, "Spontaneous autophoretic motion of isotropic particles," Phys. Fluids **25**, 061701 (2013).